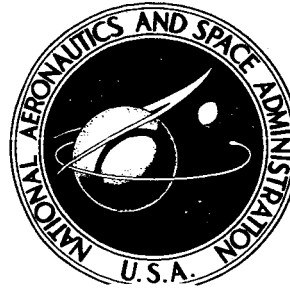


NASA CONTRACTOR  
REPORT



NASA CR-695

NASA CR-695

N67-16013

STANDARD FORM 602

(ACCESSION NUMBER)	(THRU)
32	1
(PAGES)	(CC)
CR-695	28
(NASA CR OR TMX CR AD NUMBER)	(CATEGORY)

THEORETICAL INVESTIGATION OF  
RADIANT HEAT TRANSFER IN THE  
FUEL REGION OF A GASEOUS  
NUCLEAR ROCKET ENGINE

by A. S. Kesten and N. L. Krascella

Prepared by

UNITED AIRCRAFT CORPORATION

East Hartford, Conn.

for

PRICE \$

PRICE(S) \$ 9.00

copy (HC)

copy (MF) 15

THEORETICAL INVESTIGATION OF RADIANT HEAT TRANSFER  
IN THE FUEL REGION OF A GASEOUS  
NUCLEAR ROCKET ENGINE

By A. S. Kesten and N. L. Krascella

Distribution of this report is provided in the interest of information exchange. Responsibility for the contents resides in the author or organization that prepared it.

Prepared under Contract No. NASw-847 by  
UNITED AIRCRAFT CORPORATION  
East Hartford, Conn.

for

NATIONAL AERONAUTICS AND SPACE ADMINISTRATION

## FOREWORD

An exploratory experimental and theoretical investigation of gaseous nuclear rocket technology is being conducted by the United Aircraft Corporation Research Laboratories under Contract NASw-847 with the joint AEC-NASA Space Nuclear Propulsion Office. The Technical Supervisor of the Contract for NASA is Captain W. A. Yingling (USAF). Results of the investigation conducted during the period between September 15, 1965 and September 15, 1966 are described in the following six reports (including the present report) which comprise the required fourth Interim Summary Technical Report under the Contract:

1. Krascella, N. L.: Theoretical Investigation of the Absorptive Properties of Small Particles and Heavy-Atom Gases. NASA CR-693, 1967. (Unclassified)
2. Kinney, R. B.: Theoretical Effect of Seed Opacity and Turbulence on Temperature Distributions in the Propellant Region of a Vortex-Stabilized Gaseous Nuclear Rocket (U). NASA CR-694, 1967. (report classified Confidential)
3. Kesten, A. S., and N. L. Krascella: Theoretical Investigation of Radiant Heat Transfer in the Fuel Region of a Gaseous Nuclear Rocket Engine. NASA CR-695, 1967. (Unclassified) (present report)
4. Roback, R.: Theoretical Performance of Rocket Engines Using Gaseous Hydrogen in the Ideal State at Stagnation Temperatures up to 20,000 R. NASA CR-696, 1967. (Unclassified)
5. Latham, T. S.: Nuclear Criticality Study of a Specific Vortex-Stabilized Gaseous Nuclear Rocket Engine (U). NASA CR-697, 1967. (report classified Confidential)
6. McLafferty, G. H., H. E. Bauer, and D. E. Sheldon: Preliminary Conceptual Design Study of a Specific Vortex-Stabilized Gaseous Nuclear Rocket Engine (U). NASA CR-698, 1967. (report classified Confidential)

Theoretical Investigation of Radiant Heat Transfer  
in the Fuel Region of a Gaseous Nuclear Rocket Engine

TABLE OF CONTENTS

	<u>Page</u>
SUMMARY . . . . .	1
INTRODUCTION . . . . .	2
EFFECT OF CHANGES IN IONIZATION POTENTIAL ON SPECTRAL AND MEAN ABSORPTION PROPERTIES OF NUCLEAR FUEL . . . . .	3
TEMPERATURE DISTRIBUTION IN FUEL-CONTAINMENT REGION . . . . .	5
REFERENCES . . . . .	10
LIST OF SYMBOLS . . . . .	11
FIGURES 1 through 17 . . . . .	12

Theoretical Investigation of Radiant Heat Transfer  
in the Fuel Region of a Gaseous Nuclear Rocket Engine

SUMMARY

A series of calculations were made to determine temperature distributions in the fuel-containment region of gaseous nuclear rocket engines which are based on the transfer of energy by thermal radiation from the fuel to the propellant. Temperature distributions were determined for two sets of fuel opacities; the opacities in each of these sets were calculated from an analytical heavy-atom model using two recent theoretical estimates of fuel ionization potentials. The temperatures near the centerline of the fuel-containment region were found to be high and relatively insensitive to changes in fuel opacity.

## INTRODUCTION

A number of different gaseous nuclear rocket engine concepts have been proposed in which energy is transferred from the fuel to the propellant by thermal radiation: for example, the coaxial-flow reactor described in Ref. 1 and the nuclear light bulb reactor described in Ref. 2. The temperature distribution in the fuel-containment region of such engines is dependent upon the fuel opacity characteristics. These opacity characteristics can be analytically determined using a heavy-atom model (described in Ref. 3) which requires, as a prerequisite, a knowledge of the ionization potentials of the nuclear fuel. To date, two independent theoretical estimates of the first four ionization potentials of uranium have been made (Refs. 4 and 5). The object of the study described in the following sections is to ascertain the effect of fuel opacity characteristics, determined using the heavy-atom model of Ref. 3 and the ionization potentials reported in Refs. 4 and 5, on the temperature distributions in the fuel-containment region of gaseous nuclear rocket engines of the type described in Refs. 1 and 2.

EFFECT OF CHANGES IN IONIZATION POTENTIAL ON SPECTRAL  
AND MEAN ABSORPTION PROPERTIES OF NUCLEAR FUEL

The spectral absorption coefficients and Rosseland mean opacity of nuclear fuel may be analytically estimated as a function of the wave number of the incident radiation by means of the heavy-atom model described in Ref. 3. This heavy-atom model employs a set of energy levels with constant spacing for each of four fuel ionization species. All bound-bound and bound-free transitions are allowed. The strength of each transition is described by an assumed oscillator strength distribution function. The total oscillator strength from any specified energy level to all other energy levels (bound-bound transitions) and the continuum (bound-free transition) is assigned a value of 2.0. The oscillator strength for any bound-free transition, based on a hydrogenic approximation, is assigned a value of  $8.2 \times 10^{-2}$ . The results of a study of the effect of changes in various parameters used in the heavy-atom model on the spectral and mean absorptive properties of nuclear fuel were reported in Ref. 6. These results demonstrated that the absorptive properties estimated by means of the heavy-atom model are more sensitive to changes in the ionization potentials assigned to the fuel ionization species than to other input parameters required in the fuel model.

Changes in the magnitude of the ionization potential assigned each of the fuel ionization species in the heavy-atom model alters the predicted spectral absorption coefficients and Rosseland mean opacity for three reasons:

1. By causing changes in the composition in terms of various ionization species and electrons. An increase in ionization potential decreases the number density of electrons present and increases the sum of the number densities of atoms and ions present, thereby increasing opacity.
2. By changing the distribution of oscillator strength per unit energy in the bound-bound spectral region. Such a change resulting from an increase in ionization potential might either increase or decrease the Rosseland mean opacity.
3. By changing the threshold for the bound-free transitions. An increase in ionization potential will increase the oscillator strength per unit wave number and the corresponding opacity associated with the bound-free portion of the spectrum (since the wave number range of the bound-free portion of the spectrum is reduced).

Since more heat transfer usually occurs at high wave numbers (corresponding to the bound-free portion of the spectrum) than at low wave numbers, an increase in oscillator strength at high wave numbers results in an increase in mean opacity.

The temperature distributions reported in later sections of this report are based on spectral and mean absorption results obtained using two sets of ionization potentials in the heavy-atom model. Typical spectral absorption coefficients for the nuclear fuel are given in Fig. 1 for a total pressure of 1000 atm and in Fig. 2 for 100 atm at temperatures of 10,000, 50,000, and 100,000 K (18,000, 90,000, and 180,000 R). In both figures spectral absorption coefficients shown as solid lines are based on fuel ionization potentials calculated at UAC (see Ref. 4), and those shown as dashed lines are for results based on fuel ionization potentials calculated at the Los Alamos Scientific Laboratory (see Ref. 5). It is interesting to note that the fuel ionization potentials used in Ref. 3 (6, 10, 18 and 28 ev), which were obtained by comparison with the measured ionization potentials of other high-atomic-weight atoms, are very close to those calculated in Ref. 5.

Rosseland mean opacities were calculated using the ionization potentials reported in Refs. 4 and 5 and are given by Eq. (1):

$$\alpha_R = \frac{\int_0^\infty \left( \frac{dB_\omega}{dT} \right) d\omega}{\int_0^\infty \left( \frac{1}{\alpha_\omega^*} \right) \left( \frac{dB_\omega}{dT} \right) d\omega} \quad (1)$$

Typical results are shown in Fig. 3 for several pressures between 1 and 2000 atm and for temperatures between 10,000 K (18,000 R) and 100,000 K (180,000 R). The Rosseland mean opacity for nuclear fuel computed with UAC ionization potentials (Ref. 4) are higher at all temperatures investigated than the corresponding Rosseland mean results based on the Los Alamos ionization potentials (Ref. 5). Typically, at a pressure of 100 atm, the ratio of the UAC mean opacity to Los Alamos mean opacity at a temperature of 10,000 K (18,000 R) is approximately 1.4 while at 100,000 K (180,000 R), the ratio is approximately 5.4 (see Fig. 3).



## TEMPERATURE DISTRIBUTION IN FUEL-CONTAINMENT REGION

The proper procedure for calculating the temperature distribution in the fuel-containment region of gaseous nuclear rocket engines in which radiation is the primary mode of energy transfer is different for different ranges of optical thickness of the fuel-containment region. If the fuel-containment region is relatively transparent, the temperature in the fuel-containment region will be relatively constant (assuming no convective loss of heat), and the energy radiated from the edge of the fuel-containment region will be less than that for black-body radiation at the fuel temperature. According to Ref. 7, the effective emissivity of an isothermal, relatively transparent cylinder of gas is given approximately as follows:

$$\frac{Q_6}{Q_{6_{BB}}} = 2\alpha_R r_6 \quad (2)$$

Since the radius of the fuel-containment region of gaseous nuclear rocket engines is relatively large (usually 30 cm or more), Eq. (2) is valid only for values of Rosseland mean opacity less than approximately  $0.01 \text{ cm}^{-1}$ . It can be seen from Fig. 3 that such low fuel opacities are encountered only for very low fuel pressures and very high fuel temperatures. Because the critical mass requirements of gaseous nuclear rockets will lead to relatively high pressures, Eq. (2) is of little practical use.

Calculations to determine the approximate temperature distribution in a relatively opaque cylinder of gaseous nuclear fuel are presented in Appendix I of Ref. 8. It was assumed in Ref. 8 that the opacity of the nuclear fuel was independent of radius and that the heat generation rate per unit volume was constant throughout the cylindrical fuel region. The results of these calculations indicated that the temperature at the centerline of the fuel-containment region might be two or more times the temperature at the outside edge of the fuel-containment region. However, because of the rapid variation of fuel opacity with temperature (see Fig. 3), it is difficult to choose an average value of fuel opacity to employ with the results of Ref. 8.

New calculations of the temperature distribution in the fuel-containment region have been made using two revisions of the procedures of Ref. 8. The first of these revisions consists of permitting the Rosseland mean opacity to vary as a function of the local temperature in the fuel-containment region rather than assuming a constant value as in Ref. 8. The second revision consists of assuming that the heat creation rate per unit volume is proportional to the local fuel density rather than being independent of radius as in Ref. 8. The second assumption leads to the following equation:

$$\rho_F \epsilon = - \frac{1}{r} \frac{d}{dr} \left( \frac{16}{3} \frac{\sigma T^3}{a_R} r \frac{dT}{dr} \right) \quad (3)$$

The left side of Eq. (3) represents the energy created per unit volume per unit time, with the quantity  $\epsilon$  being proportional to neutron flux. The right side of Eq. (3) represents the change in heat flux with radial position as indicated by the diffusion equation. In obtaining solutions to Eq. (3), the fuel-containment region is taken to be a long, hollow cylinder as shown in Fig. 4. The temperature and heat flux are specified at the outside edge of the fuel region. In addition, the temperature gradient is taken as zero at the inside edge of the fuel region which is assumed to have a radius equal to 0.1 times the radius at the outside edge of the fuel-containment region. Since there is no heat generation inside the inside edge of the fuel-containment region, the temperature at this station is equal to the centerline temperature. All calculations assume pure fuel in the fuel-containment region (i.e., the presence of hydrogen propellant, which will, to some extent, diffuse into the fuel-containment region, is neglected).

In most cases calculated for high fuel pressures, the temperature gradient at the outside edge of the fuel-containment region has been found to be extremely large. A simple expression for this temperature gradient can be obtained as follows for the case in which the heat flux at the edge of the fuel-containment region is equal to black-body heat flux for the temperature at the edge of the fuel-containment region. Black-body heat flux is given by the following equation:

$$Q_{6BB} = \sigma T_6^4 \quad (4)$$

According to the diffusion equation,

$$Q_6 = - \frac{16}{3} \frac{\sigma T_6^3}{a_R} \left( \frac{dT}{dr} \right)_6 \quad (5)$$

Therefore, the temperature gradient at the edge of the fuel is given by

$$\left( \frac{dT}{dr} \right)_6 = - \frac{3}{16} a_R T_6 \quad (6)$$

Temperature gradients at the edge of the fuel-containment region calculated using Eq. (6) and the opacity information developed using the Los Alamos ionization potentials (see Fig. 3) are shown in Fig. 5. Although the temperature gradient is small at low pressures and high temperatures, extremely large temperature gradients are

obtained at low temperatures and high pressures. Since the temperature gradient is proportional to Rosseland mean opacity, temperature gradients determined using opacities calculated from UAC ionization potentials would be higher than those shown in Fig. 5 and determined using opacities calculated from Los Alamos ionization potentials (see Fig. 3).

Four typical temperature distributions in the fuel-containment region calculated from Eq. (3), two for each set of ionization potentials, are given in Fig. 6. For each of these temperature distributions, the pressure was assumed to be 10 atm, the radius of the fuel-containment region was assumed to be 10 ft, and the heat flux at the edge of the fuel-containment region was assumed to be  $1.23 \times 10^6$  Btu/sec-ft<sup>2</sup> (black-body heat flux for a temperature of 40,000 R). Two calculations were made for each set of ionization potentials; it was assumed in one calculation that the temperature at the edge of the fuel-containment region was equal to the black-body temperature corresponding to the assumed heat flux (40,000 R), while in the second calculation this temperature was assumed to be 60,000 R. It can be seen that the difference in assumed temperature at the outside edge of the fuel-containment region makes almost no difference in the temperature distribution inside a radius of 95 percent of the radius of the fuel-containment region. This result stems from the high temperature gradients indicated in Fig. 5 and the rapid change of radiation thermal conductivity with temperature due both to the change of Rosseland mean opacity with temperature indicated in Fig. 3 and the  $T^3$  term in the diffusion equation.

The solutions presented in Fig. 6 were obtained using a computing machine program in which 1000 intervals were employed between the inside and outside edges of the fuel-containment region. This machine calculation program gave inconsistent answers for some calculations in which the temperature gradient at the edge of the fuel-containment region was extremely high (see Fig. 5). For such cases, the steep temperature gradient led to an unrealistically high temperature rise in the first calculation step even though the radius interval was only  $10^{-3}$  times the fuel region radius. In such instances, the calculations were rerun using a higher assumed temperature at the outside edge of the fuel-containment region. Such an assumed change in temperature will have almost no effect on the true temperature distribution over most of the fuel-region volume as indicated by the results shown in Fig. 6.

Results such as those shown in Fig. 6 can be generalized on the basis of the following reasoning. Consider a temperature-vs-radius solution for a given fuel pressure, a given heat flux at the edge of the fuel region, and a given fuel radius. Consider also a second temperature distribution which has the same temperature variation with  $r/r_g$  as the first temperature distribution and the same fuel pressure, but a fuel radius,  $r_g$ , equal to  $G$  times the fuel radius in the first temperature distribution. The temperature gradients and, by the diffusion approximation, the heat fluxes in the second temperature distribution will be  $1/G$  times those in the first temperature distribution. Thus the total heat flow (equal to the product of

circumference and heat flux) at any given value of  $r/r_6$  will be the same for the two temperature distributions. The heat flow in both temperature distributions will be proportional to the amount of fuel inside of a given value of  $r/r_6$ , but the proportionality factor which describes neutron flux ( $\epsilon$  in Eq. (3)) will be  $1/G^2$  times as great for the second temperature distribution as the first (i.e., Eq. (3) will be satisfied for both temperature distributions). Thus the dimensionless temperature distribution ( $T$  vs  $r/r_6$ ) at a given pressure is determined by specifying only the heat transfer rate per unit length of fuel cylinder,  $2\pi r_6 Q_6$ . Since this result relies on arguments involving the diffusion approximation, it is valid only when the diffusion approximation is valid, which requires approximately that the heat flux at the edge of the fuel region be less than black-body heat flux at the temperature at the edge of the fuel region.

Results of calculations similar to those whose results are illustrated in Fig. 6 are given in Figs. 7 through 14. The temperature at the centerline (inside edge of the fuel-containment region), calculated using the Los Alamos ionization potentials, is plotted as a function of heat transfer rate per unit length in Figs. 7 and 8 for values of  $T_6$  less than and greater than 100,000 R, respectively. The results of similar calculations using the UAC ionization potentials are shown in Figs. 9 and 10. The average density within the fuel-containment region, calculated using the Los Alamos ionization potentials, is shown as a function of heat transfer rate per unit length in Figs. 11 and 12 for average fuel densities less than and greater than  $10^{-2}$  gm/cm<sup>3</sup>, respectively. Average fuel densities calculated using the UAC ionization potentials are shown in Figs. 13 and 14. The influence of the two different sets of ionization potentials on the variation with pressure of fuel centerline temperatures and average fuel densities is shown more directly in Figs. 15 and 16. In addition, a comparison of the effect of average fuel density on fuel centerline temperatures for the two sets of ionization potentials is illustrated in Fig. 17. It may be noted that, although the opacities calculated from the two sets of ionization potentials are considerably different, the calculated values of fuel centerline temperatures are fairly close at a given average fuel density and heat transfer rate per unit length at the edge of the fuel-containment region.

The use of the results shown in Fig. 16 and 17 can be illustrated by the following example. Consider a gaseous nuclear rocket engine with a fuel cylinder having a diameter of 1.0 meter (3.28 ft) and a length of 3.0 meters (9.83 ft). Assume that the total power to be radiated from the cylindrical surface of the fuel region (neglecting axial radiation from the ends) is 10,000 mw ( $9.5 \times 10^6$  Btu/sec). Assume also that the neutron moderator surrounding the fuel-containment region results in the requirement of 10 kg of nuclear fuel to achieve criticality. Since the volume of the fuel-containment region is  $2.35 \times 10^6$  cm<sup>3</sup>, the required average critical fuel density is  $(10^4 \text{ gm}) / (2.35 \times 10^6 \text{ cm}^3) = 4.25 \times 10^{-3} \text{ gm/cm}^3 = 0.265 \text{ lb/ft}^3$ . Also the heat transfer rate per unit length of fuel cylinder is  $(9.5 \times 10^6 \text{ Btu/sec}) / (9.83 \text{ ft}) = 0.968 \times 10^6 \text{ Btu/sec-ft}$ . Entering Fig. 16 with these quantities leads to required fuel pressures of 170 and 195 atm using the Los Alamos and UAC ionization potentials,

respectively. Entering Fig. 17 leads to centerline temperatures of 81,000 and 93,000 R using the Los Alamos and UAC ionization potentials, respectively. Since it will be impossible to prevent the diffusion of some foreign gas (hydrogen propellant in the concept of Ref. 1 or buffer gas in the concept of Ref. 2) into the fuel-containment region, the total gas pressure must be greater than that due to the fuel alone. Also the foreign gas will raise the opacity above that of the fuel alone and result in an increase in centerline temperature. However, this latter effect should be small since the opacity of gases such as hydrogen is much less than that of nuclear fuel at the same temperature and pressure (Ref. 3).

## REFERENCES

1. Rom, F. E. and R. G. Ragsdale: Advanced Concepts for Nuclear Rocket Propulsion. Nuclear Rocket Propulsion, NASA SP-20, December 1962, pp. 3-15.
2. McLafferty, G. H.: Absorption of Thermal Radiation in the Transparent Wall of a Nuclear Light Bulb Rocket Engine. UARL Report UAR-E63 presented at AIAA Second Propulsion Joint Specialist Conference, June 13-16, 1966.
3. Krascella, N. L.: Theoretical Investigation of the Spectral Opacities of Hydrogen and Nuclear Fuel. Air Force Systems Command Report RTD-TDR-63-1101 prepared by UAC Research Laboratories under Contract AF 04(611)-8189, November 1963.
4. Williamson, H. A., H. H. Michels, and S. B. Schneiderman: Theoretical Investigation of the Lowest Five Ionization Potentials of Uranium. UAC Research Laboratories Report D-910099-2 prepared under Contract NASw-847, September 1965.
5. Waber, J. T., D. Liberman, and D. T. Cromer: Unpublished Theoretical Ionization Potentials for Uranium. Los Alamos Scientific Laboratory, received June 1966.
6. Krascella, N. L.: Theoretical Investigation of the Opacity of Heavy-Atom Gases. UAC Research Laboratories Report D-910092-4 prepared under Contract NASw-847, September 1965.
7. McLafferty, G. H.: Approximate Limitations on the Specific Impulse of Advanced Nuclear Rocket Engines Due to Nozzle Coolant Requirements. UARL Report D-110224-1, April 1965.
8. McLafferty, G. H., H. H. Michels, T. S. Latham, and R. Roback: Analytical Study of Hydrogen Turbopump Cycles for Advanced Nuclear Rockets. UARL Report D-910093-19 prepared under Contract NASw-847, September 1965.

# LIST OF SYMBOLS

$Q_{\omega}^*$	Spectral absorption coefficient with stimulated emission included, $\text{cm}^{-1}$
$Q_R$	Rosseland mean opacity, $\text{cm}^{-1}$
$I_F^0, I_F^+, I_F^{++}, I_F^{+++}$	Ionization potentials, ev or $\text{cm}^{-1}$
$G$	Factor used in discussion in text
$P$	Pressure, atm
$Q$	Radiant heat flux, $\text{Btu/sec-ft}^2$
$Q_6$	Radiant heat flux at edge of fuel-containment region, $\text{Btu/sec-ft}^2$
$Q_{6\text{bb}}$	Black-body heat flux for temperature equal to temperature at edge of fuel-containment region, $\text{Btu/sec-ft}^2$
$r$	Distance from centerline of cylindrical fuel region, ft or cm
$r_6$	Radius of fuel-containment region, ft or cm
$T$	Temperature, deg R or deg K
$\epsilon$	Energy generation rate in fuel, $\text{Btu/lb-sec}$
$\rho_F$	Fuel density, $\text{lb/ft}^3$
$\overline{\rho_{F_6}}$	Average fuel density within fuel cylinder, $\text{lb/ft}^3$
$\sigma$	Stephan Boltzmann constant, $0.48 \times 10^{-12} \text{ Btu/sec-ft}^2\text{-(deg R)}^4$
$\omega$	Wave number, $\text{cm}^{-1}$

COMPARISON OF THE EFFECT OF WAVE NUMBER ON THE SPECTRAL ABSORPTION COEFFICIENT OF NUCLEAR FUEL FOR DIFFERENT IONIZATION POTENTIALS USED IN THE HEAVY-ATOM MODEL AT 100 ATM TOTAL PRESSURE

CURVE	IONIZATION POTENTIALS								IONIZATION POTENTIALS FROM REF
	$I_{F0}$		$I_{F+}$		$I_{F++}$		$I_{F+++}$		
	ev	CM <sup>-1</sup>	ev	CM <sup>-1</sup>	ev	CM <sup>-1</sup>	ev	CM <sup>-1</sup>	
————	6.1	49210	17.1	137946	38.8	313000	65.6	529195	4
-----	6.11	49290	11.46	92450	17.94	144724	31.14	251209	5

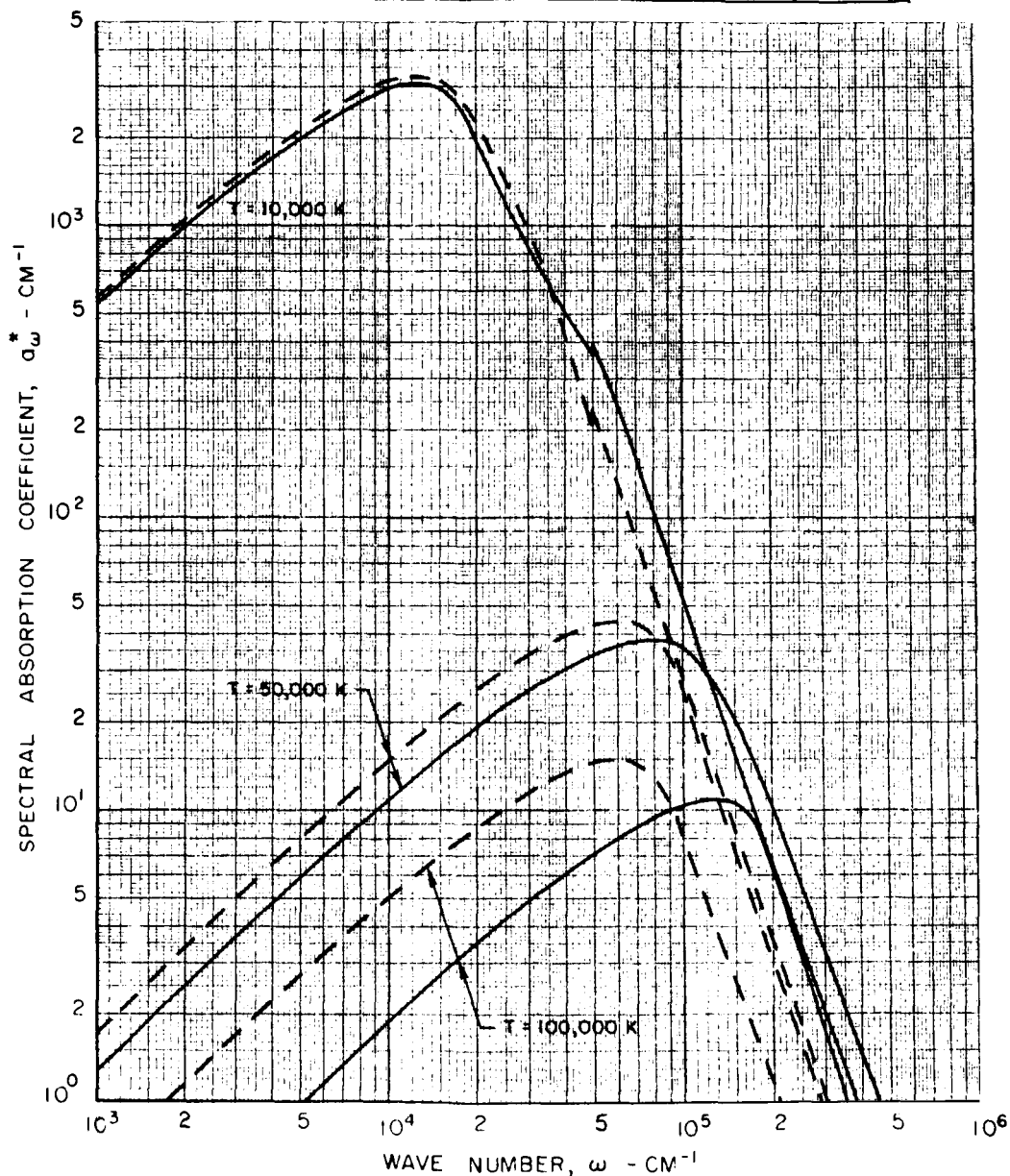
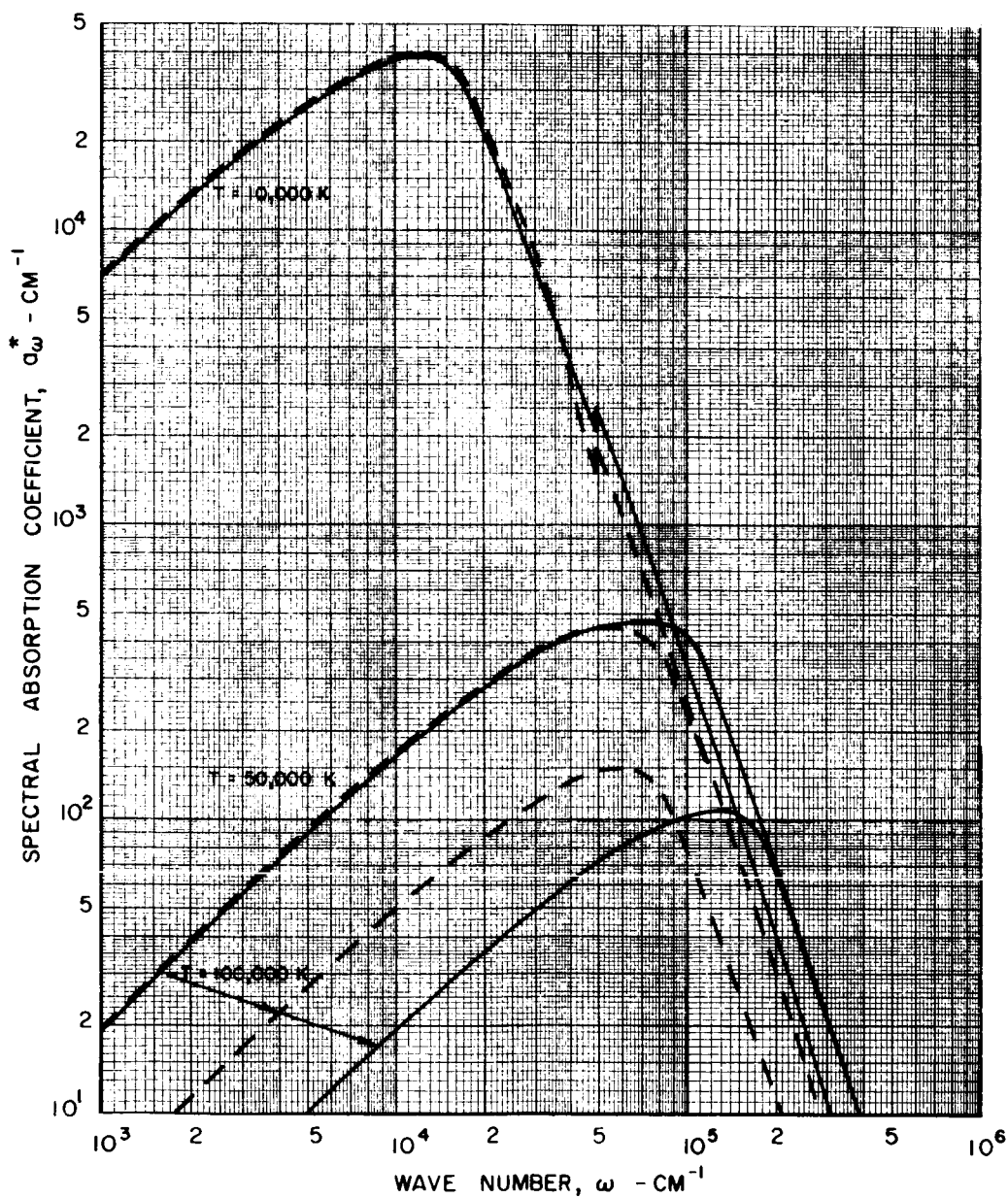




FIG. 2

COMPARISON OF THE EFFECT OF WAVE NUMBER ON THE SPECTRAL ABSORPTION COEFFICIENT OF NUCLEAR FUEL FOR DIFFERENT IONIZATION POTENTIALS USED IN THE HEAVY-ATOM MODEL AT 1000 ATM TOTAL PRESSURE

CURVE	IONIZATION POTENTIALS								IONIZATION POTENTIALS FROM REF
	$I_{pe}$		$I_{p+}$		$I_{p++}$		$I_{p+++}$		
	ev	CM <sup>-1</sup>	ev	CM <sup>-1</sup>	ev	CM <sup>-1</sup>	ev	CM <sup>-1</sup>	
————	6.1	49210	17.1	137946	38.8	313000	65.6	529195	4
-----	6.11	49290	11.46	92450	17.94	144724	31.14	251209	5



COMPARISON OF THE EFFECT OF TEMPERATURE ON THE  
ROSSELAND MEAN OPACITY OF NUCLEAR FUEL FOR DIFFERENT  
IONIZATION POTENTIALS USED IN THE HEAVY-ATOM MODEL

CURVE	IONIZATION POTENTIALS								IONIZATION POTENTIALS FROM REF
	$I_{F0}$		$I_{F+}$		$I_{F++}$		$I_{F+++}$		
	ev	CM <sup>-1</sup>	ev	CM <sup>-1</sup>	ev	CM <sup>-1</sup>	ev	CM <sup>-1</sup>	
—————	6.1	49210	17.1	137946	38.8	313000	65.6	529195	4
-----	6.11	49290	11.46	92450	17.94	144724	31.14	251209	5

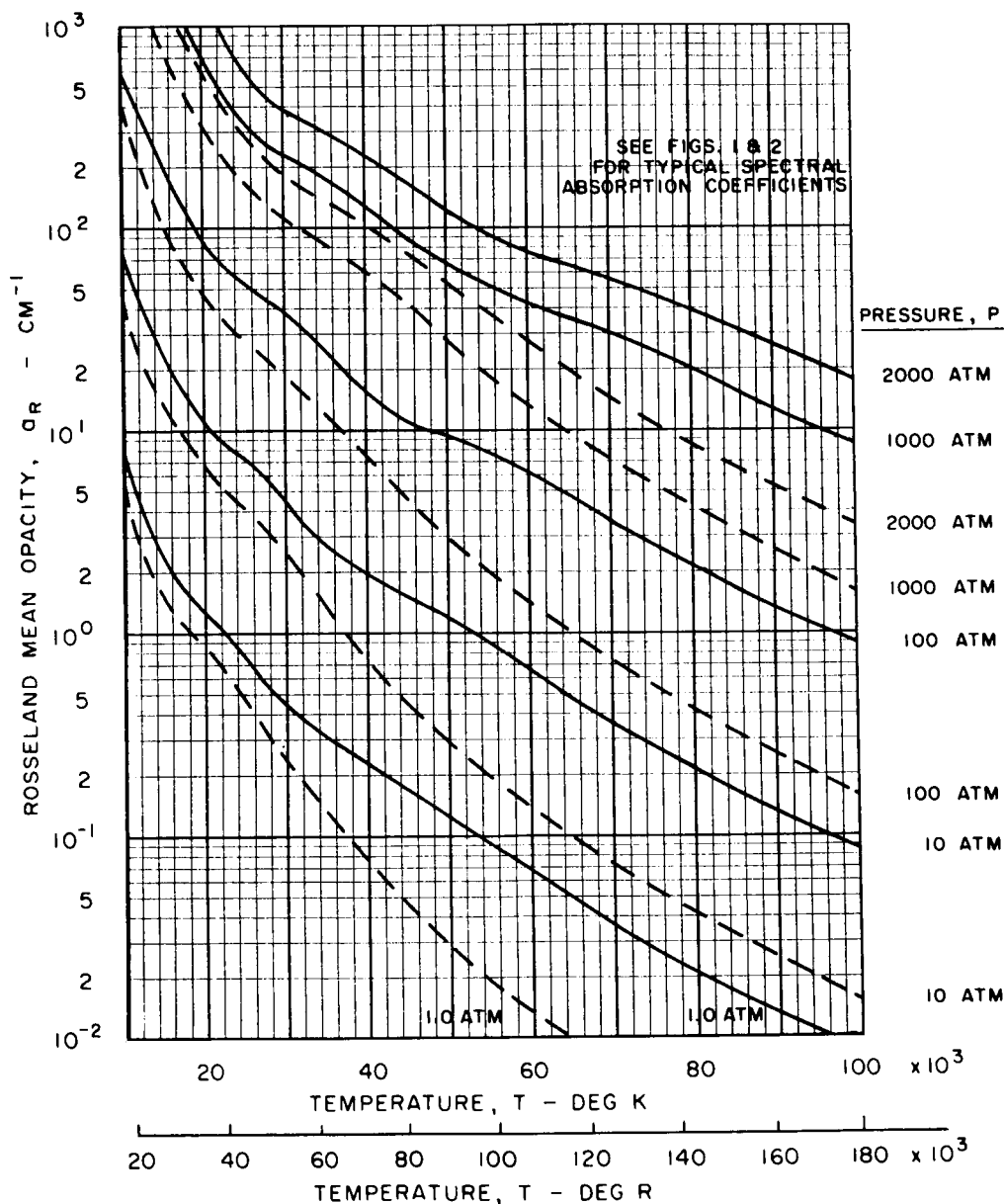


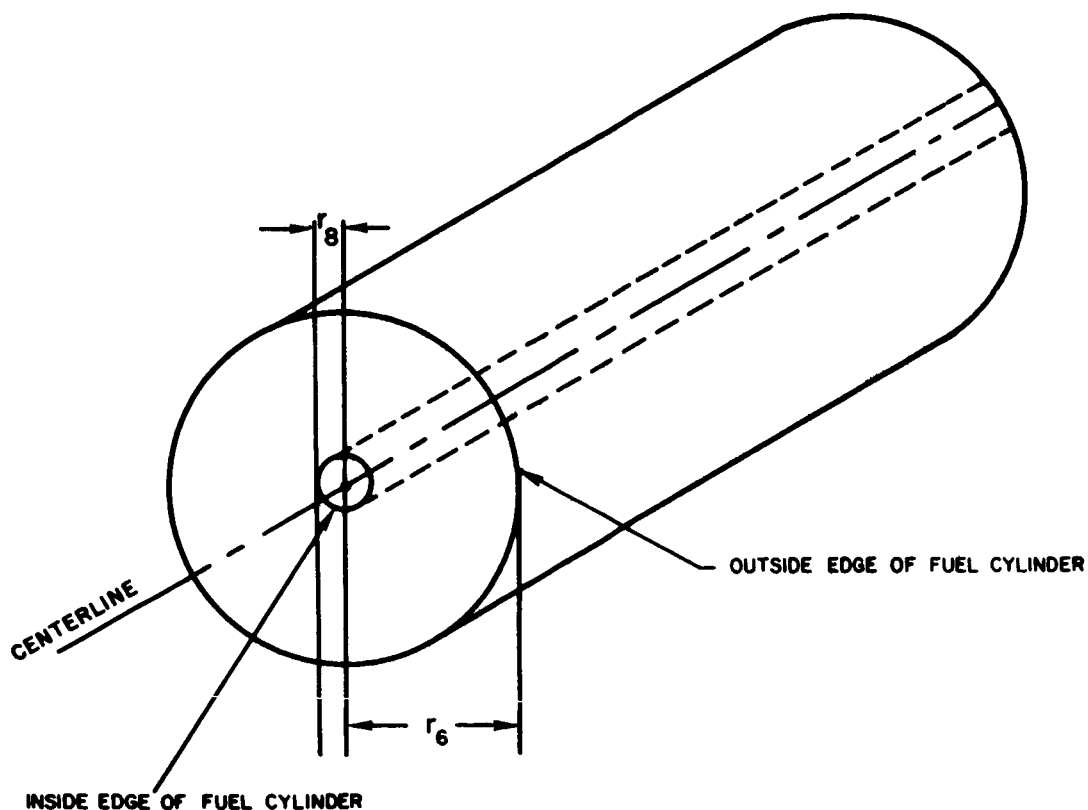
FIG. 4

## SKETCH OF FUEL CYLINDER USED IN TEMPERATURE DISTRIBUTION CALCULATIONS

FUEL PRESSURE ASSUMED CONSTANT BETWEEN  $r_6$  AND  $r_8$

LOCAL HEAT GENERATION RATE PER UNIT VOLUME ASSUMED PROPORTIONAL  
TO LOCAL FUEL DENSITY (I.E. CONSTANT NEUTRON FLUX)

END EFFECTS NEGLECTED (INFINITE LENGTH)



# TEMPERATURE GRADIENT AT EDGE OF FUEL CYLINDER FOR CASE IN WHICH HEAT FLUX EQUALS BLACK-BODY HEAT FLUX

IONIZATION POTENTIALS								IONIZATION POTENTIALS FROM REF.
$I_{F^0}$		$I_{F^+}$		$I_{F^{++}}$		$I_{F^{+++}}$		
ev	CM <sup>-1</sup>	ev	CM <sup>-1</sup>	ev	CM <sup>-1</sup>	ev	CM <sup>-1</sup>	
6.11	49290	11.46	92450	17.94	144724	31.14	251209	
								5

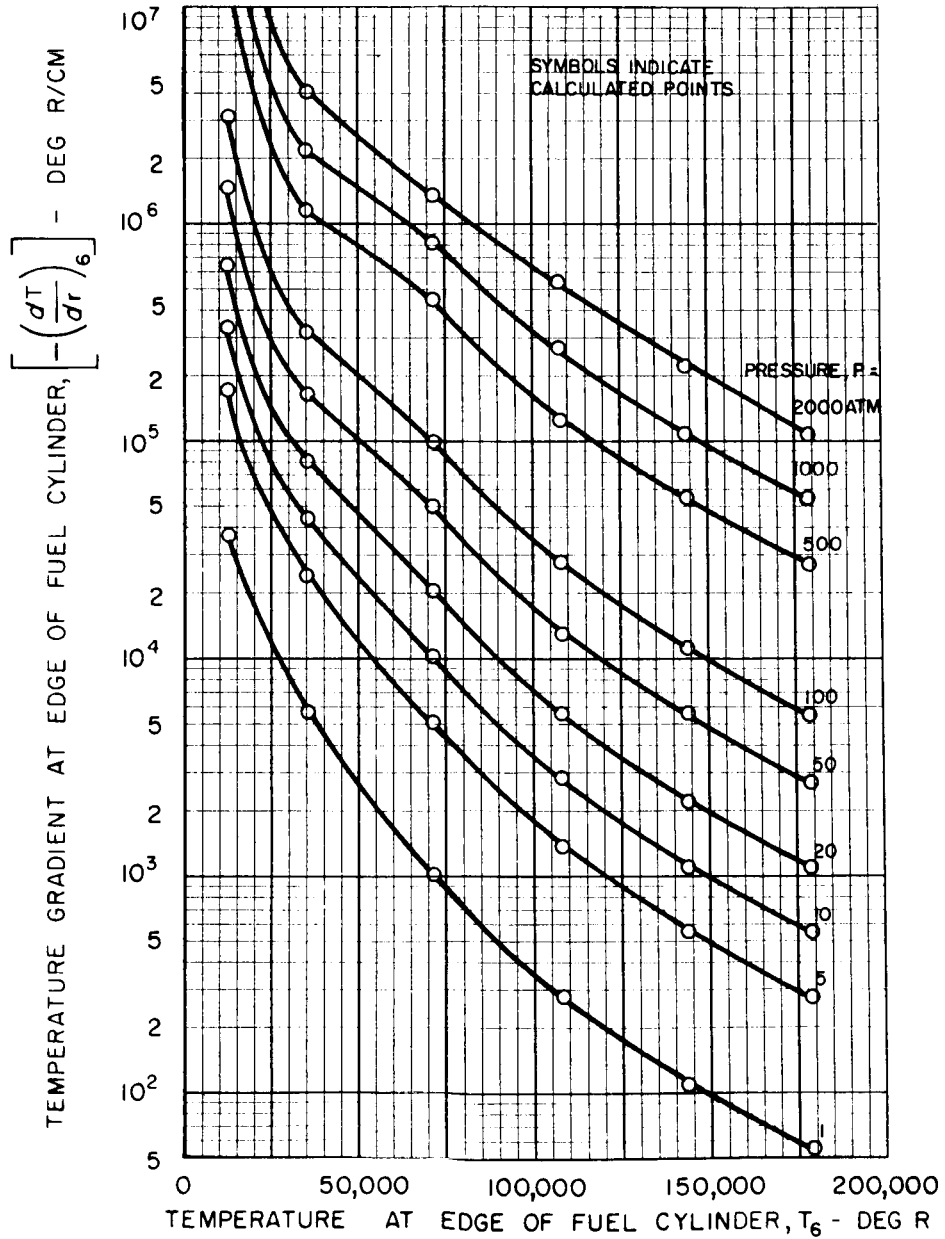


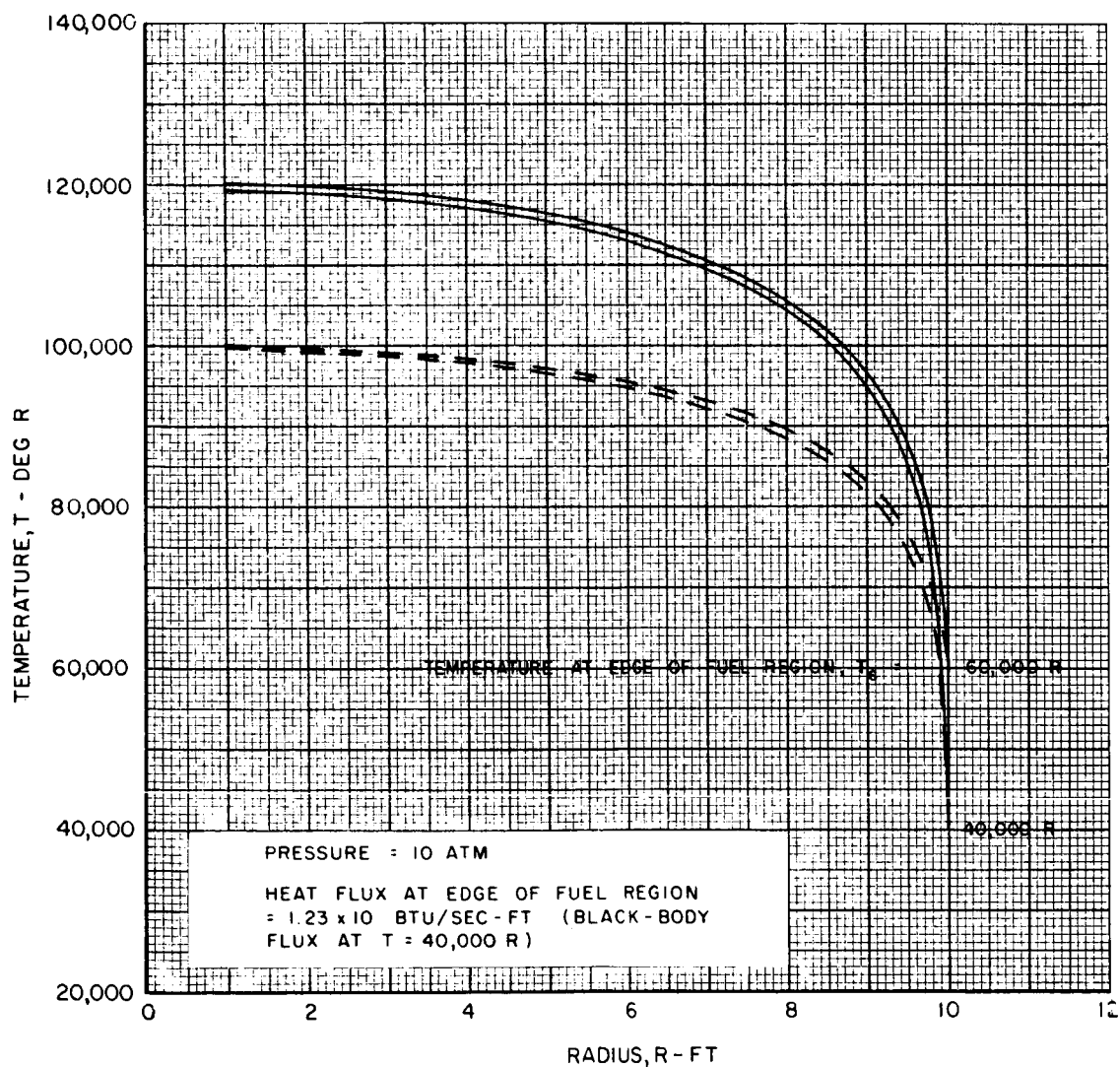


FIG. 6

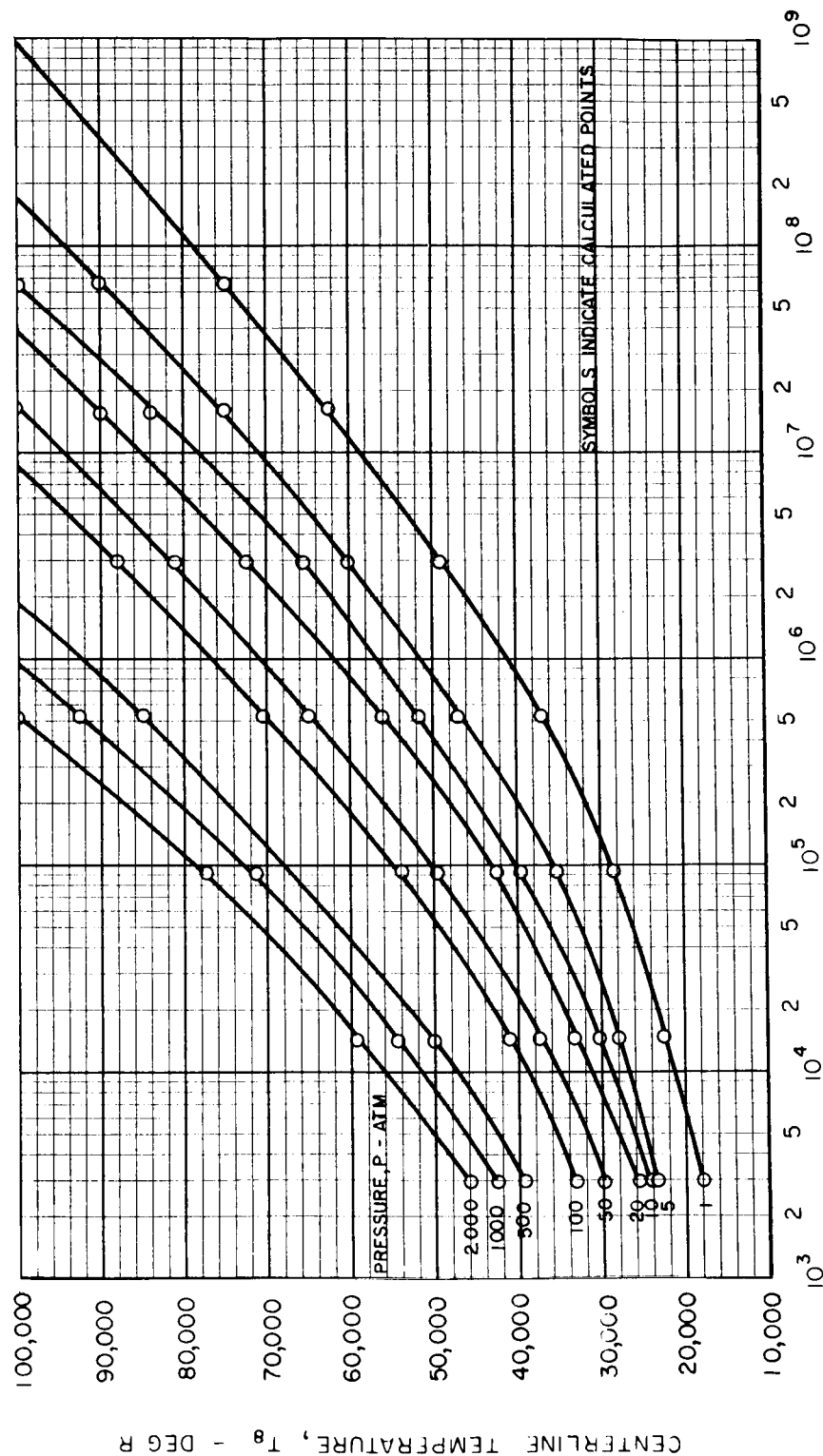
# TYPICAL CALCULATED TEMPERATURE DISTRIBUTIONS IN FUEL REGION

CURVE	IONIZATION POTENTIALS								IONIZATION POTENTIALS FROM REF
	$I_{F^0}$		$I_{F^+}$		$I_{F^{++}}$		$I_{F^{+++}}$		
	ev	CM <sup>-1</sup>	ev	CM <sup>-1</sup>	ev	CM <sup>-1</sup>	ev	CM <sup>-1</sup>	
	6.1	49210	17.1	137946	38.8	313000	65.6	529195	4
	6.11	49290	11.46	92450	17.94	144724	31.14	251209	5



# EFFECT OF HEAT TRANSFER RATE PER UNIT LENGTH OF FUEL CYLINDER ON CENTERLINE TEMPERATURES FOR CENTERLINE TEMPERATURES LESS THAN 100,000 R FOR LOS ALAMOS IONIZATION POTENTIALS

IONIZATION POTENTIALS				IONIZATION POTENTIALS FROM REF.				
$I_{F0}$		$I_{F+}$		$I_{F++}$				
e v	CM <sup>-1</sup>	e v	CM <sup>-1</sup>	e v	CM <sup>-1</sup>			
6.11	49290	11.46	92450	17.94	144724	31.14	251209	5



HEAT TRANSFER RATE PER UNIT LENGTH OF FUEL CYLINDER,  $2\pi Q_6$  - BTU/SEC-FT

# EFFECT OF HEAT TRANSFER RATE PER UNIT LENGTH OF FUEL CYLINDER ON CENTERLINE TEMPERATURES FOR CENTERLINE TEMPERATURES GREATER THAN 100,000 R FOR LOS ALAMOS IONIZATION POTENTIALS

IONIZATION POTENTIALS						IONIZATION POTENTIALS FROM REF.		
$I_{F0}$		$I_{F+}$		$I_{F++}$				
eV	CM <sup>-1</sup>	eV	CM <sup>-1</sup>	eV	CM <sup>-1</sup>			
6.11	49290	11.46	92450	17.94	144724	31.14	251209	5

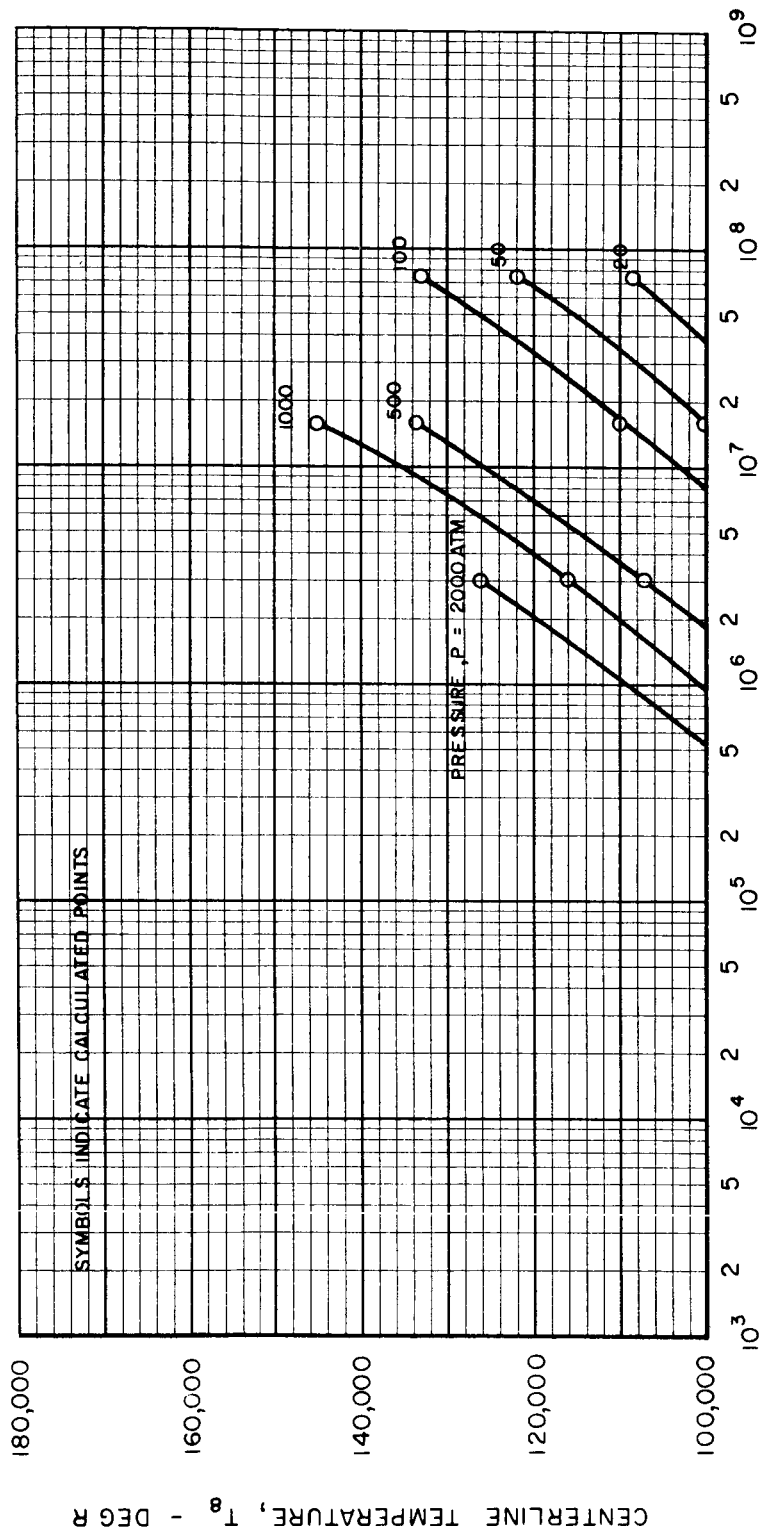
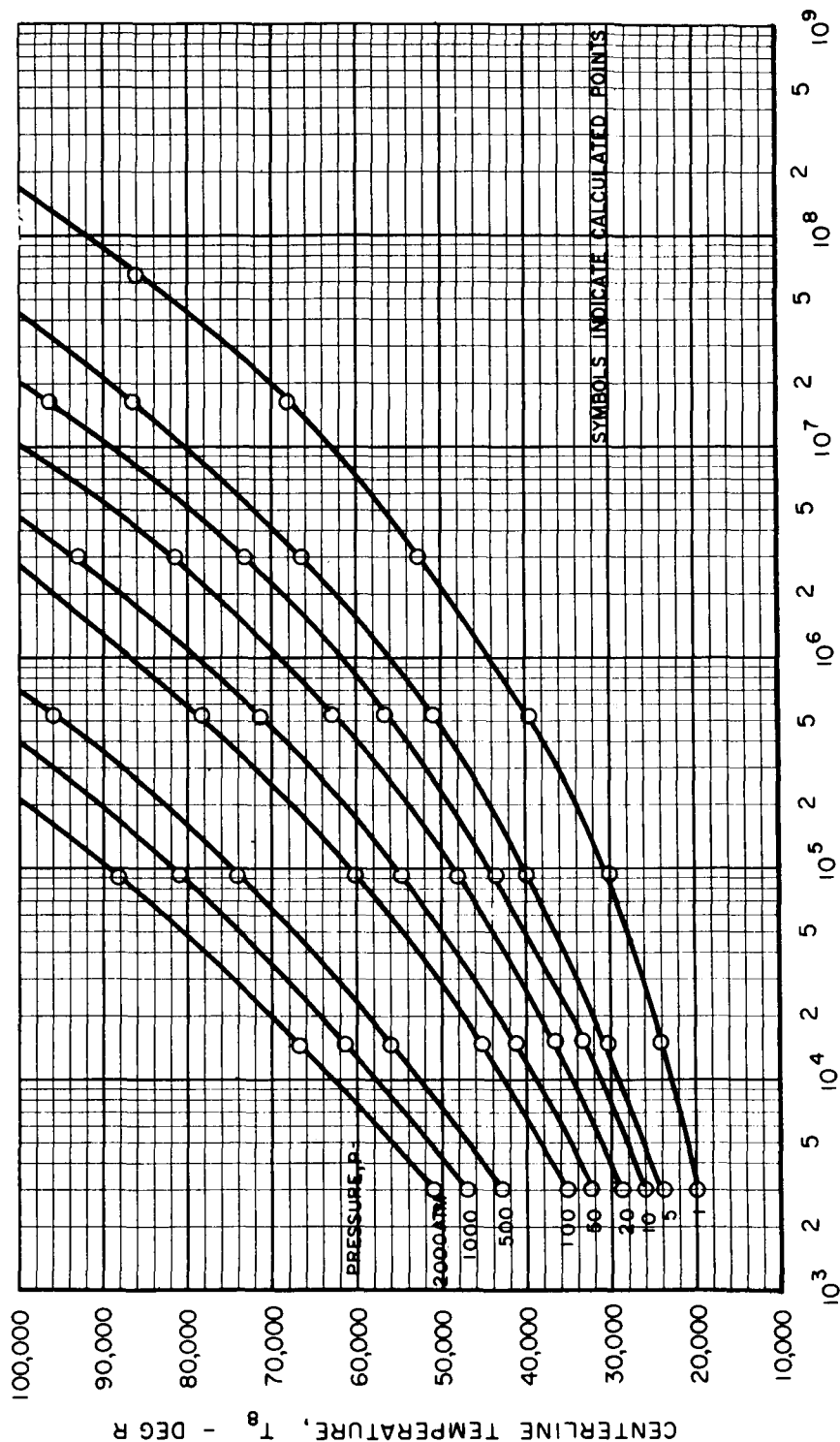


FIG. 8

# EFFECT OF HEAT TRANSFER RATE PER UNIT LENGTH OF FUEL CYLINDER ON CENTERLINE TEMPERATURES FOR CENTERLINE TEMPERATURES LESS THAN 100,000 R FOR UAC IONIZATION POTENTIALS

IONIZATION POTENTIALS						IONIZATION POTENTIALS FROM REF.
$I_{p0}$		$I_{p00}$		$I_{p000}$		
ev	CM <sup>-1</sup>	ev	CM <sup>-1</sup>	ev	CM <sup>-1</sup>	4
6.1	49210	17.1	137946	38.8	313000	
				65.6	529195	



HEAT TRANSFER RATE PER UNIT LENGTH OF FUEL CYLINDER,  $2\pi r_6 Q_6$  - BTU/SEC-FT



# EFFECT OF HEAT TRANSFER RATE PER UNIT LENGTH OF FUEL CYLINDER ON CENTERLINE TEMPERATURES FOR CENTERLINE TEMPERATURES GREATER THAN 100,000 R FOR UAC IONIZATION POTENTIALS

SYMBOLS INDICATE CALCULATED POINTS

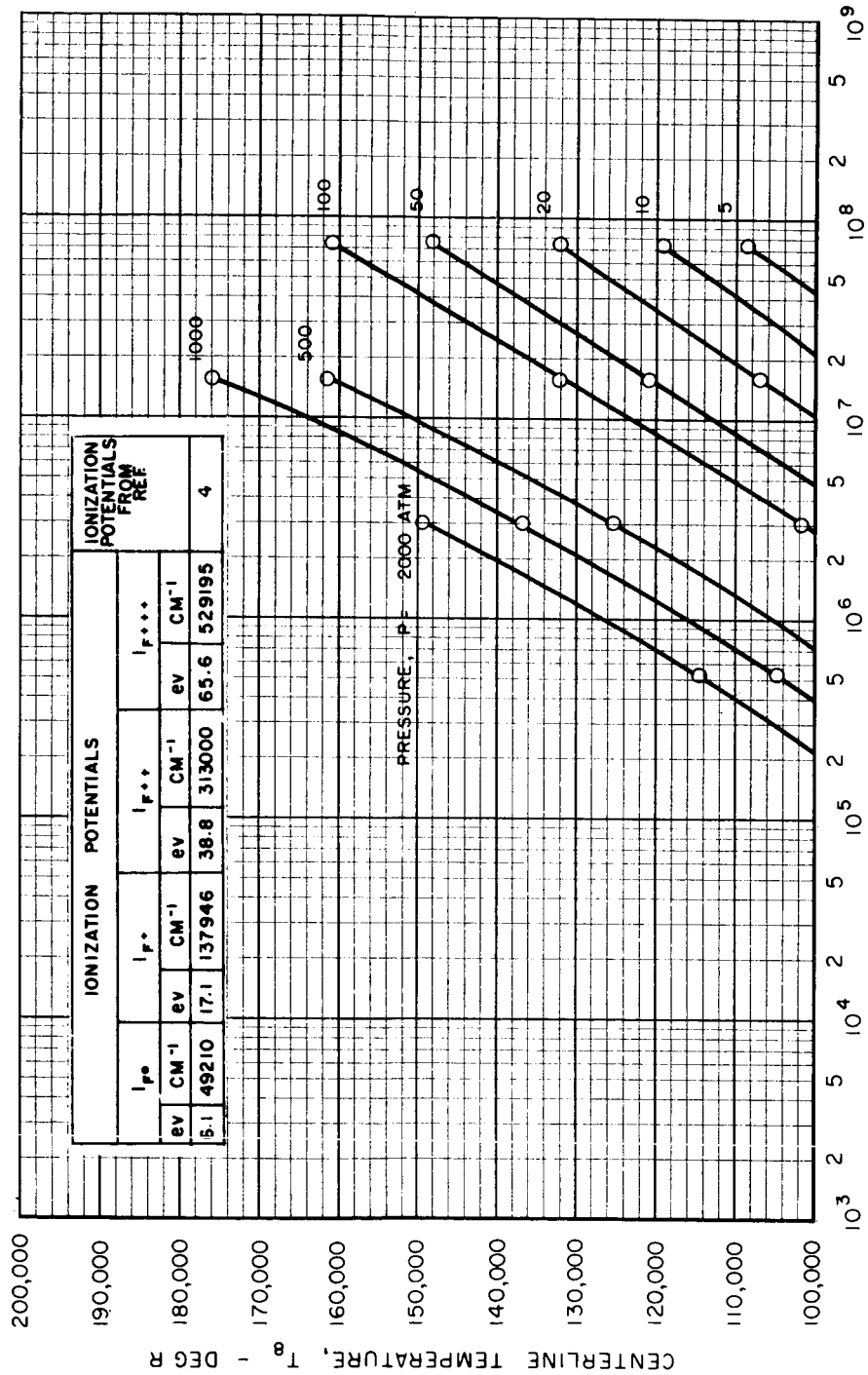


FIG. 10

EFFECT OF HEAT TRANSFER RATE PER UNIT LENGTH OF FUEL CYLINDER  
ON AVERAGE FUEL DENSITY FOR DENSITIES LESS THAN  
 $10^{-2}$  GM/CM<sup>3</sup> FOR LOS ALAMOS IONIZATION POTENTIALS

IONIZATION POTENTIALS							IONIZATION POTENTIALS FROM REF.	
$I_F^0$		$I_F^+$		$I_F^{++}$		$I_F^{+++}$		
ev	CM <sup>-1</sup>	ev	CM <sup>-1</sup>	ev	CM <sup>-1</sup>			CM <sup>-1</sup>
6.11	49290	11.46	92450	17.94	144724	31.14	251209	5

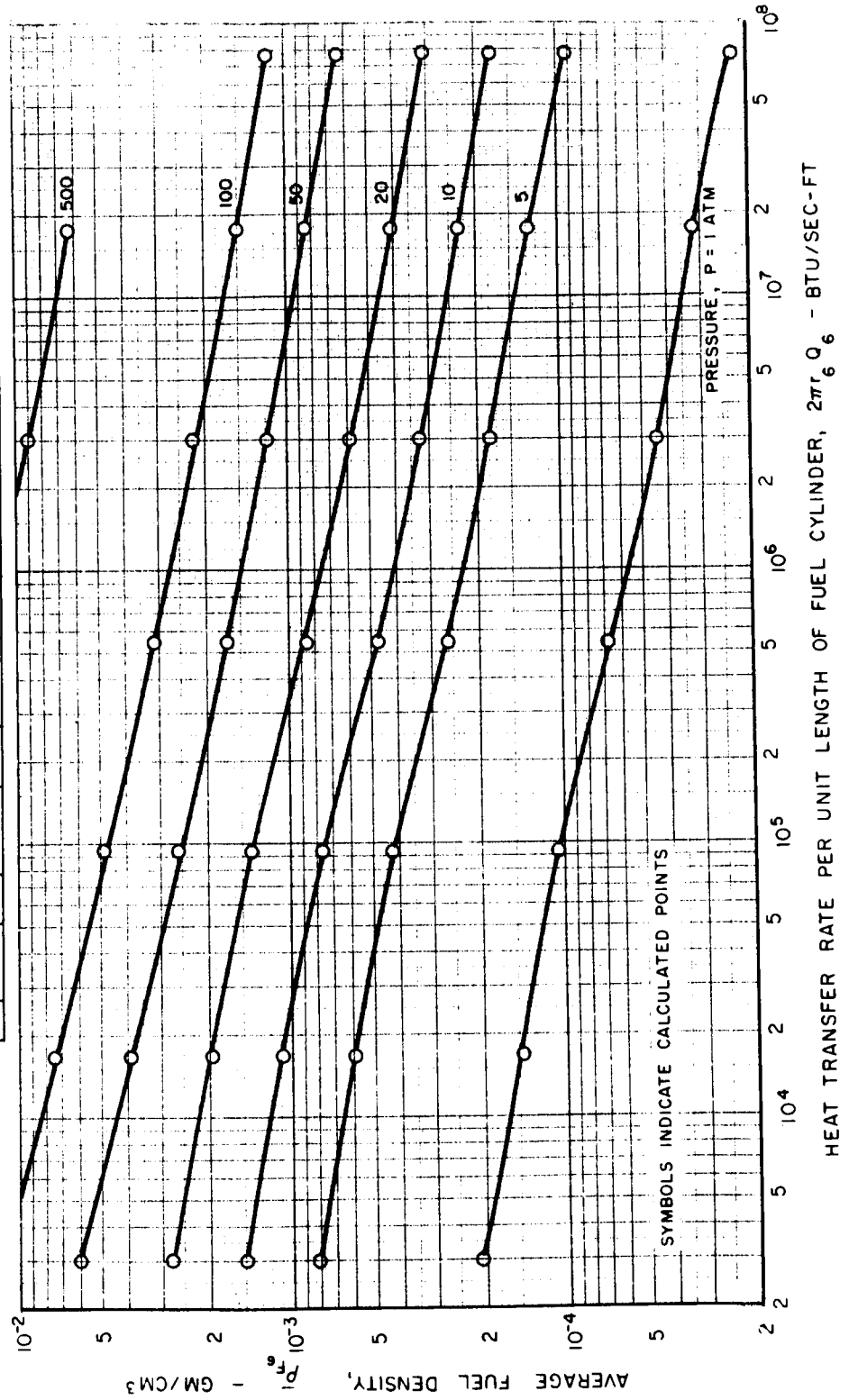
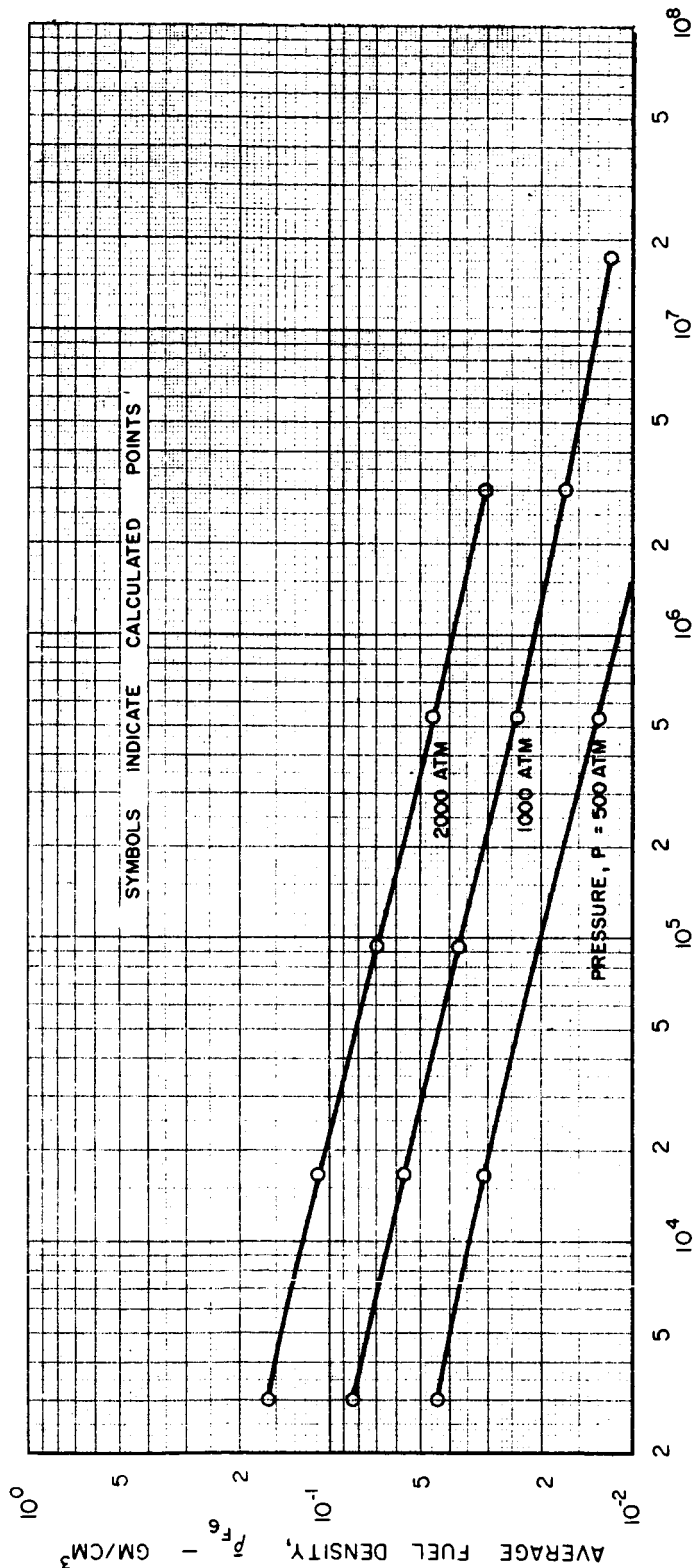


FIG. 11

# EFFECT OF HEAT TRANSFER RATE PER UNIT LENGTH OF FUEL CYLINDER ON AVERAGE FUEL DENSITY FOR DENSITIES GREATER THAN $10^{-2}$ GM/CM<sup>3</sup> FOR LOS ALAMOS IONIZATION POTENTIALS

IONIZATION POTENTIALS						IONIZATION POTENTIALS FROM REF.		
$I_{p0}$		$I_{p0}$		$I_{p0}$				
ev	CM <sup>-1</sup>	ev	CM <sup>-1</sup>	ev	CM <sup>-1</sup>			
6.11	49290	11.46	92450	17.94	144724	31.14	251209	5



HEAT TRANSFER RATE PER UNIT LENGTH OF FUEL CYLINDER,  $2\pi r_6 Q_6$  - BTU/SEC-FT

EFFECT OF HEAT TRANSFER RATE PER UNIT LENGTH  
OF FUEL CYLINDER ON AVERAGE FUEL DENSITY  
FOR DENSITIES LESS THAN  $10^{-2}$  GM/CM<sup>3</sup>  
FOR UAC IONIZATION POTENTIALS

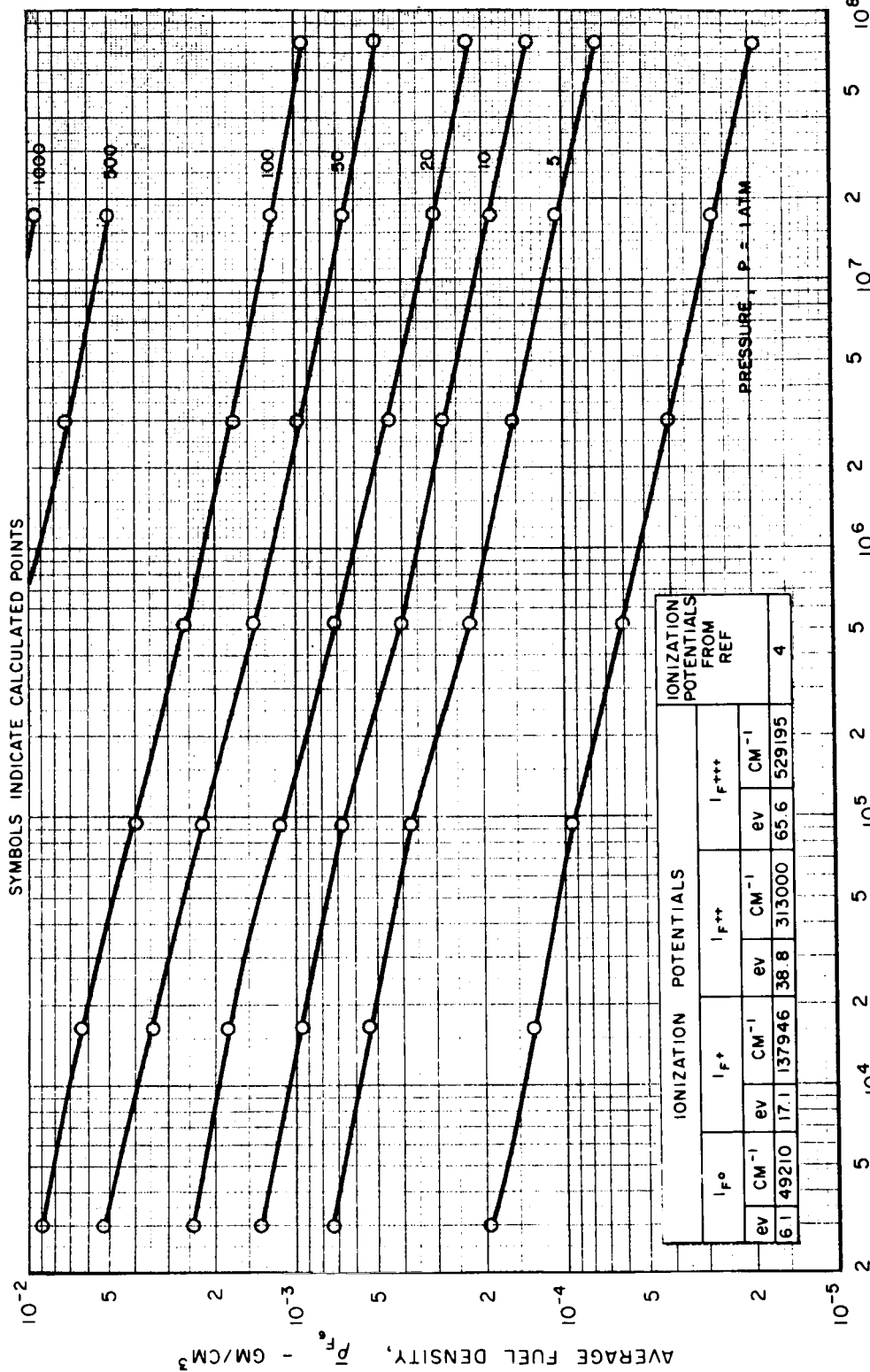


FIG. 13

# EFFECT OF HEAT TRANSFER RATE PER UNIT LENGTH OF FUEL CYLINDER ON AVERAGE FUEL DENSITY FOR DENSITIES GREATER THAN $10^{-2} \text{GM/CM}^3$ FOR UAC IONIZATION POTENTIALS

IONIZATION POTENTIALS							IONIZATION POTENTIALS FROM REF	
$I_{p0}$		$I_{p1}$		$I_{p2}$		$I_{p3}$		
ev	cm <sup>-1</sup>	ev	cm <sup>-1</sup>	ev	cm <sup>-1</sup>			ev
6.1	49210	17.1	137946	38.8	313000	65.6	529195	4

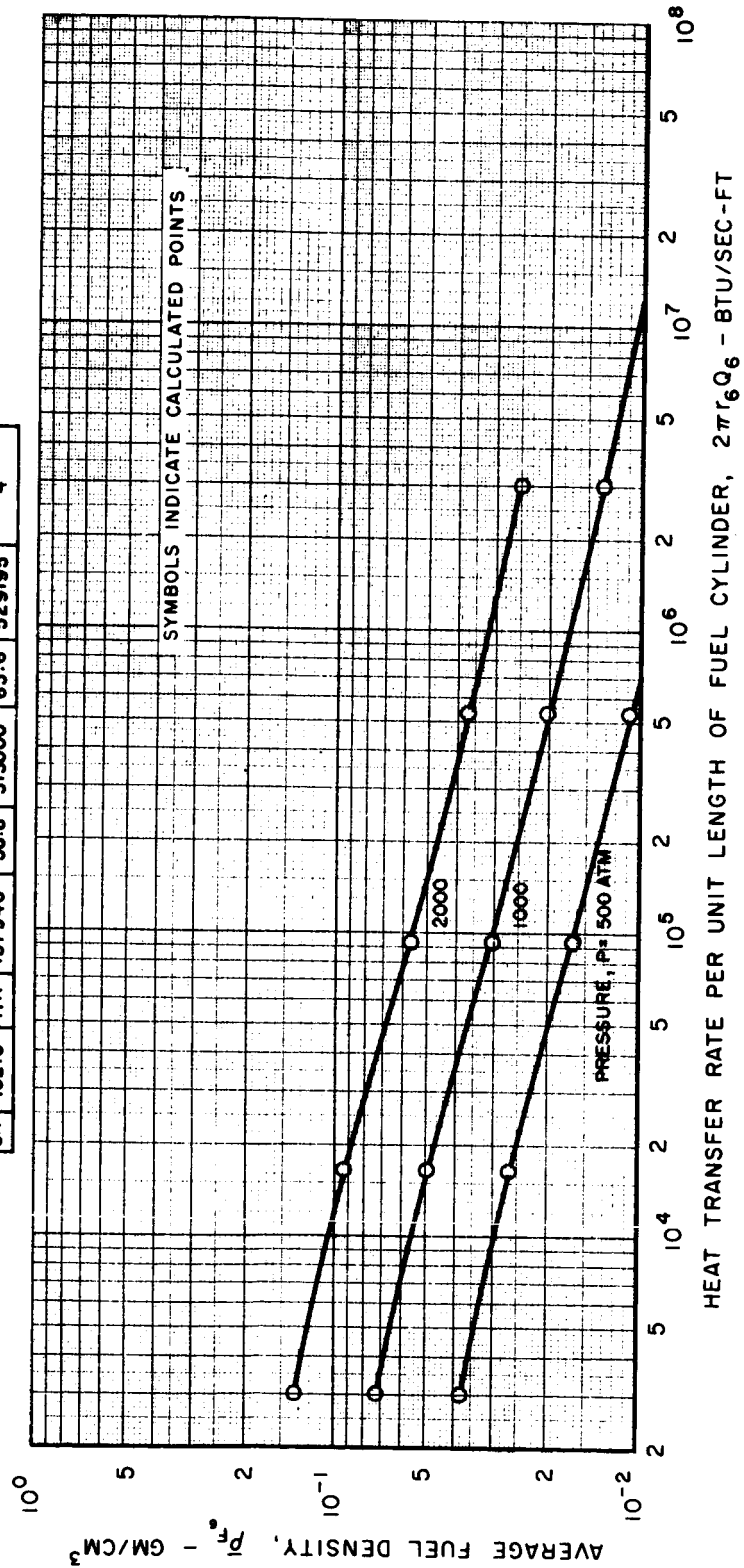


FIG. 14

FIG. 15

COMPARISON OF THE EFFECT OF PRESSURE ON FUEL CENTERLINE  
TEMPERATURES FOR DIFFERENT IONIZATION POTENTIALS USED  
IN THE HEAVY - ATOM MODEL

CURVE	IONIZATION POTENTIALS								IONIZATION POTENTIALS FROM REF
	$I_{p0}$		$I_{p1}$		$I_{p2}$		$I_{p3}$		
	ev	CM <sup>-1</sup>	ev	CM <sup>-1</sup>	ev	CM <sup>-1</sup>	ev	CM <sup>-1</sup>	
—	6.1	49210	17.1	137946	38.8	313000	65.6	529195	4
- - -	6.11	49290	11.46	92450	17.94	144724	31.14	251209	5

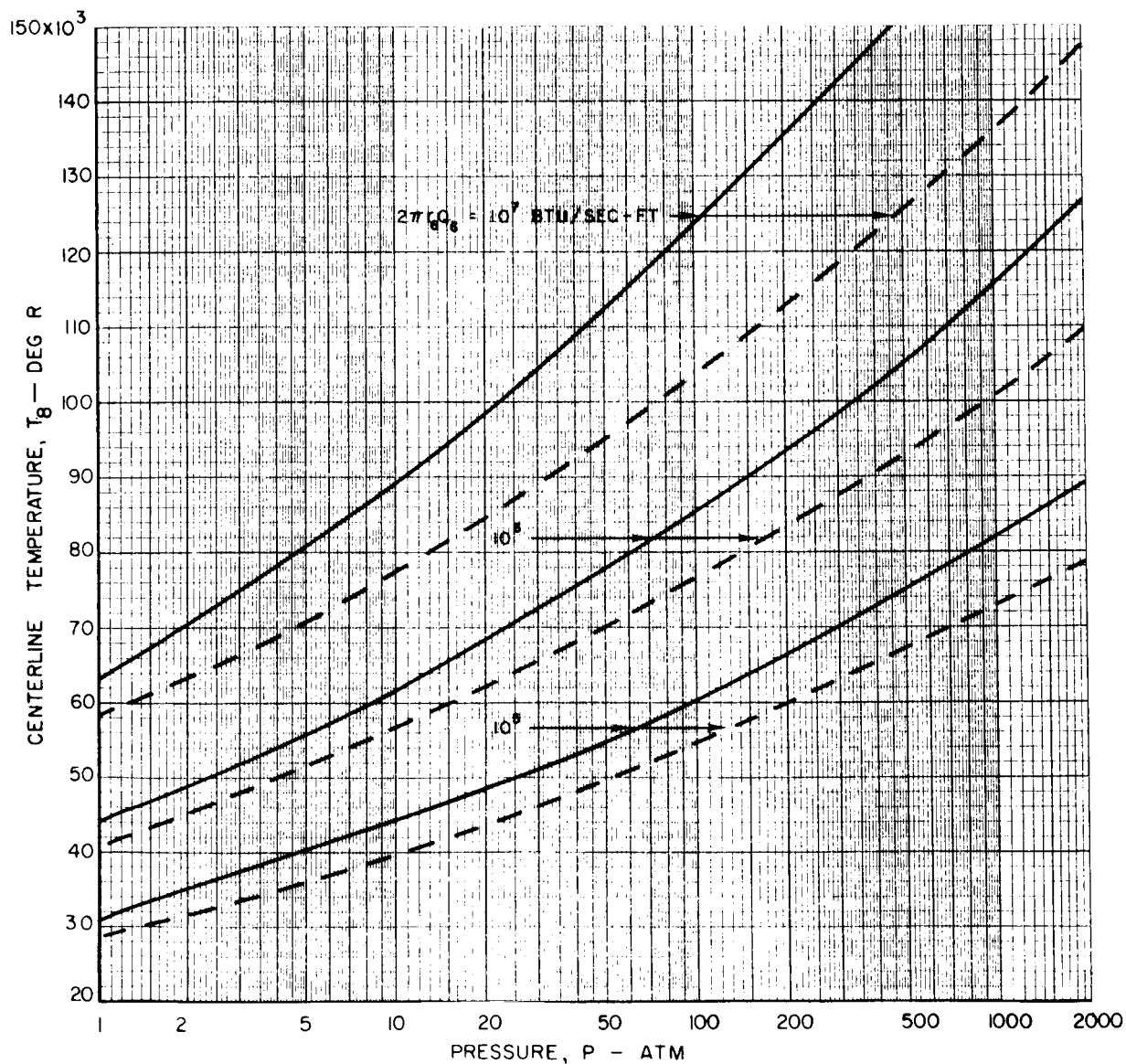
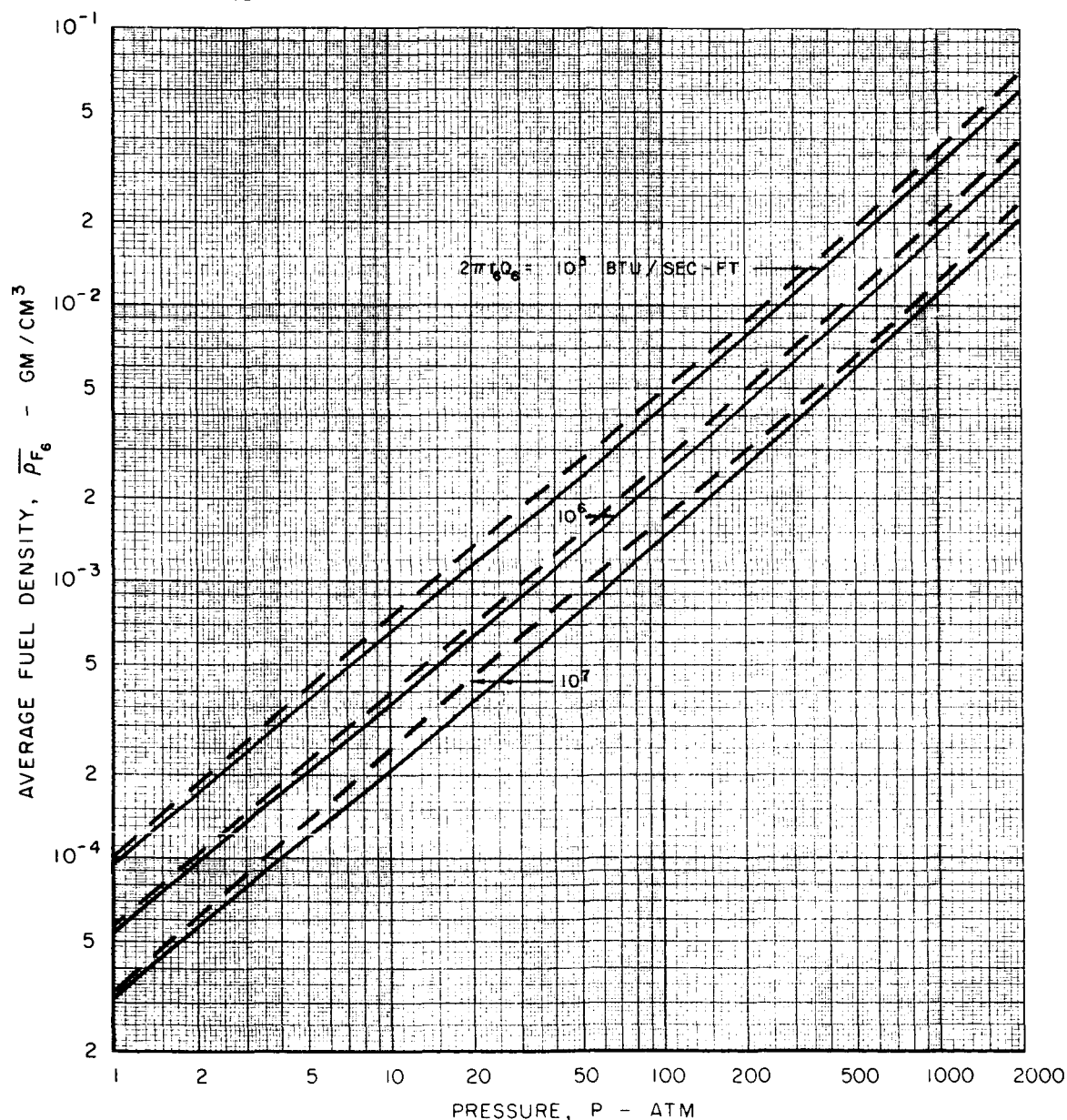


FIG. 16

COMPARISON OF THE EFFECT OF PRESSURE ON AVERAGE  
FUEL DENSITIES FOR DIFFERENT IONIZATION POTENTIALS  
USED IN THE HEAVY-ATOM MODEL

CURVE	IONIZATION POTENTIALS								IONIZATION POTENTIALS FROM REF
	$I_{F0}$		$I_{F+}$		$I_{F++}$		$I_{F+++}$		
	ev	CM <sup>-1</sup>	ev	CM <sup>-1</sup>	ev	CM <sup>-1</sup>	ev	CM <sup>-1</sup>	
————	6.1	49210	17.1	137946	38.8	313000	65.6	529195	4
-----	6.11	49290	11.46	92450	17.94	144724	31.14	251209	5



COMPARISON OF THE EFFECT OF AVERAGE FUEL DENSITY ON FUEL CENTERLINE TEMPERATURES FOR DIFFERENT IONIZATION POTENTIALS USED IN THE HEAVY ATOM MODEL

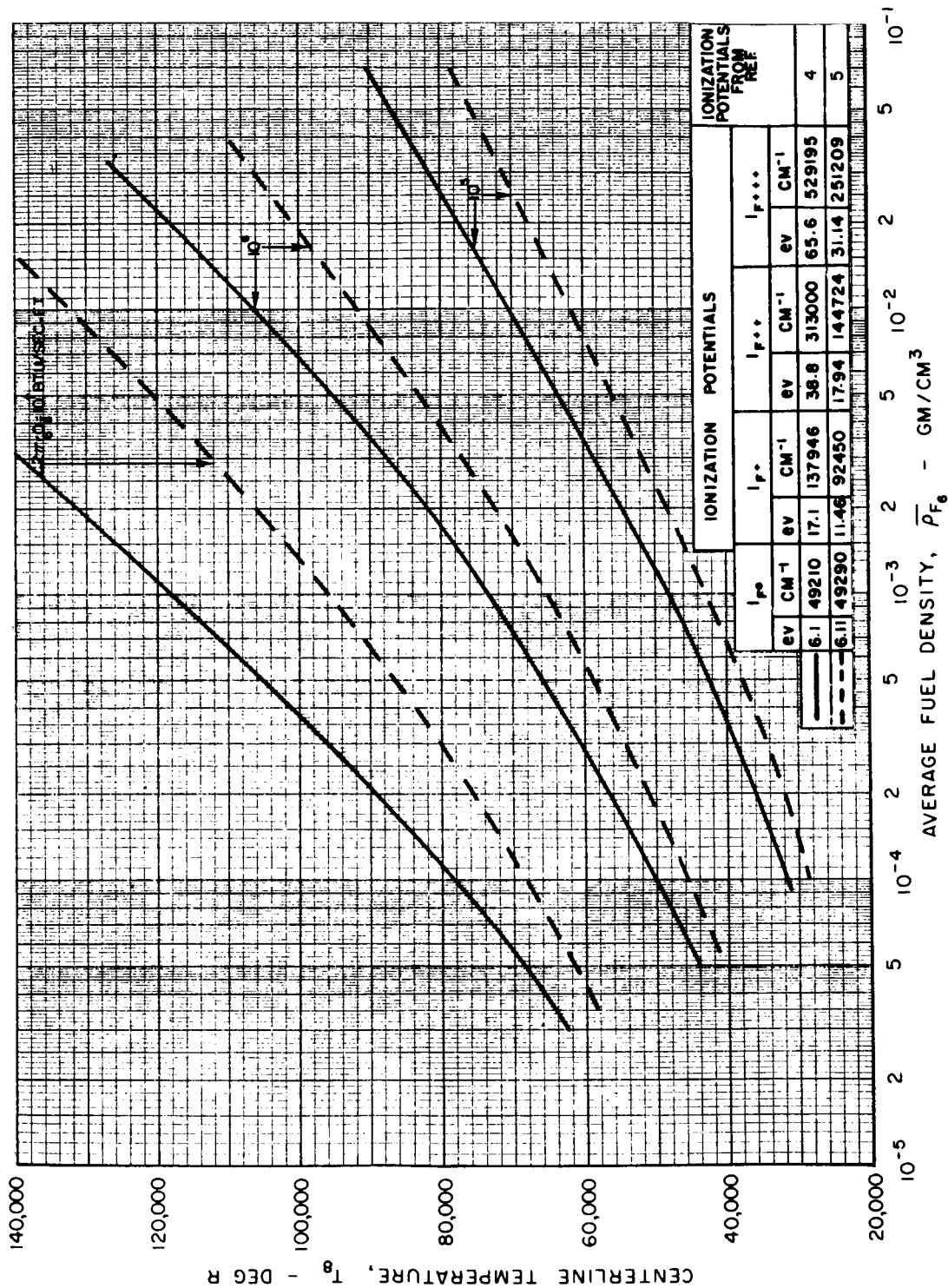


FIG. 17



00972  
107 up  
26-1-67

*"The aeronautical and space activities of the United States shall be conducted so as to contribute . . . to the expansion of human knowledge of phenomena in the atmosphere and space. The Administration shall provide for the widest practicable and appropriate dissemination of information concerning its activities and the results thereof."*

—NATIONAL AERONAUTICS AND SPACE ACT OF 1958

## NASA SCIENTIFIC AND TECHNICAL PUBLICATIONS

**TECHNICAL REPORTS:** Scientific and technical information considered important, complete, and a lasting contribution to existing knowledge.

**TECHNICAL NOTES:** Information less broad in scope but nevertheless of importance as a contribution to existing knowledge.

**TECHNICAL MEMORANDUMS:** Information receiving limited distribution because of preliminary data, security classification, or other reasons.

**CONTRACTOR REPORTS:** Technical information generated in connection with a NASA contract or grant and released under NASA auspices.

**TECHNICAL TRANSLATIONS:** Information published in a foreign language considered to merit NASA distribution in English.

**TECHNICAL REPRINTS:** Information derived from NASA activities and initially published in the form of journal articles.

**SPECIAL PUBLICATIONS:** Information derived from or of value to NASA activities but not necessarily reporting the results of individual NASA-programmed scientific efforts. Publications include conference proceedings, monographs, data compilations, handbooks, sourcebooks, and special bibliographies.

*Details on the availability of these publications may be obtained from:*

SCIENTIFIC AND TECHNICAL INFORMATION DIVISION  
NATIONAL AERONAUTICS AND SPACE ADMINISTRATION  
Washington, D.C. 20546